POLYGONAL PARTITION-BASED HYPERSPECTRAL IMAGE CLASSIFICATION WITH SINGLE LABELED SAMPLE

Shuo Zhang, Xiaohui Wei, Xudong Kang, Puhong Duan, Shutao Li

College of Electrical and Information Engineering, Hunan University, Changsha, China.

IGARSS 2021 - 2021 IEEE International Geoscience and Remote Sensing Symposium | 978-1-6654-0369-6/21/$31.00 ©2021 IEEE | DOI: 10.1109/IGARSS47720.2021.9553067

ABSTRACT

It is well known that classification accuracy highly relies on the number of labeled samples. However, it is difficult to obtain sufficient labeled samples in real-world applications. To solve this issue, a novel hyperspectral image (HSI) classification method based on polygonal partition is proposed for crop mapping. This method only needs single sample per class as an initial training set. Specifically, multiscale polygonal partition is applied on the first three components of the HSI. Then, a spectral similarity-based sample expansion method is proposed to obtain more labeled samples. Next, a pixel-wise classifier, the support vector machine (SVM), is used to acquire an initial classification result. Finally, classification result is further optimized according to the partition maps. Experimental results show that classification performance of the proposed method is satisfactory even when the number of labeled sample is single for each class.

***Index Terms*—** Hyperspectral image classification, sample expansion, polygonal partition, single sample, crop mapping.

1. INTRODUCTION

Hyperspectral image classification is a classic and popular research topic in remote sensing community which can help people find the desired objects. In recent years, numerous classification methods with different framework have been advocated for agricultural application [1–3]. However, the amount of labeled training samples is a crucial factor for classification which limits the development of different classification methods in practical application.

To address this issue, an efficient way is to construct the discriminative features of original image. Feature extraction methods can increase the separability of samples belonging to different objects and perform well when the number of training samples is limited. For example, a multi-scale total variation method is proposed to extract discriminative structural features from HSIs in [4]. This method can effectively decrease the influence of complex texture patterns and the inner-class differences. In [5], a modified generative adversarial network (GAN) is proposed to train a feature extractor without supervision. The designed network can extracts high-level spectral and spatial features with better invariance.

Furthermore, many interesting classification frameworks have been developed to solve the small sample size problem, such as semi-supervised based method [6, 7] and active learning (AL) based method [8, 9]. Semi-supervised based methods aim to automatically enlarge the amount of training set from a few labeled samples. For instance, Wang *et al.* [6] construct a spatial-spectral graph to propagate labels to unlabeled samples, which can update the training set. In [7], Tan *et al.* select the most informative unlabeled samples based on breaking ties technology, then combine spatial neighborhood information with two classifiers to determine the labels of unlabeled samples. Besides, the AL-based methods are sample confidence based interactive training expansion techniques. Li *et al.* [8] extract the spatial and spectral information by using loopy belief propagation, and gets new samples via an AL strategy based on the conditional marginal of the unlabeled samples. In [9], empirical risk minimization principle is generalized to the AL setting. This method adopts the maximum mean discrepancy to constrain the distribution of the labeled samples and combines discriminative information to query unlabeled samples.

Although these methods mentioned above can achieve satisfactory classification accuracy when the number of training set is relatively small, the classification performance tends to decrease dramatically when the number of training sample is single. Furthermore, the homogeneity in the same land cover cannot well retained especially for farmland scene. In this paper, considering the advantage that the polygon partition technique can provide accurate object boundaries, a novel classification method is proposed for crop mapping with single training sample. Specifically, the boundaries of different objects are obtained by using polygon partition methods. Then, the amount of training sample is enlarged according to the similarities between inter- and intra- partition region. Finally, the spectral classifier is used to evaluate the classification performance.

This paper is supported by the Major Program of the National Natural Science Foundation of China (No. 61890962), the National Natural Science Foundation of China (No.61601179), the Natural Science Foundation of Hunan Province (No. 2019JJ50036), the Fund of Key Laboratory of Visual Perception and Artificial Intelligence of Hunan Province (No. 2018TP1013) and the scientific research project of Hunan Education Department (NO. 19B105).

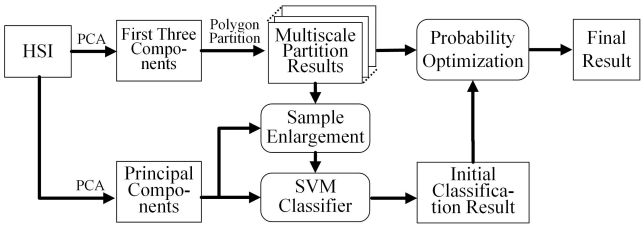

Fig. 1. The flowchart of proposed method.

2. PROPOSED CLASSIFICATION ALGORITHM

Fig.1 presents the flowchart of the proposed classification method. The specific steps are presented below.

2.1. Polygonal Partition

In this paper, Kinetic polygonal partitioning of images (KIPPI) proposed by Bauchet *et al.* is exploited to generate different scale polygons of the input. KIPPI is a kinetic approach which can partition image into polygons by extending predetected line-segments. After extracting line-segments from image, KIPPI adopts global regularization to correct imprecisions and reduce the occurrence of skinny cells, it can be formulated by minimizing the energy:

$$U(\mathrm{x}) = (1-\lambda)H(\mathrm{x}) + \lambda V(\mathrm{x}) \tag{1}$$

where $\mathbf{x} = (x_1, \ldots, x_n), x_i \in [-\theta_{\max}, \theta_{\max}]$ is a configuration of perturbations operated on the n line-segments, $H(\mathrm{x})$ and $V(\mathrm{x})$ represent data term and pairwise potential respectively, and $\lambda \in [0,1]$ is a weighting parameter. $H(\mathrm{x})$ discourages strong angle deviations with respect to their initial orientation:

$$H(\mathrm{x}) = \frac{1}{n}\sum_{i=1}^{n}\left(\frac{x_i}{\theta_{\max}}\right)^2 \tag{2}$$

$V(\mathrm{x})$ encourages pairs of spatially-close line-segments which are nearly-parallel or nearly-orthogonal to be exactly parallel or orthogonal:

$$V(\mathrm{x}) = \frac{1}{\sum_{i=1}^{n}\sum_{j>i}\mu_{ij}}\sum_{i=1}^{n}\sum_{j>i}\mu_{ij}\frac{|\theta_{ij} - x_i + x_j|}{4\theta_{\max}} \tag{3}$$

where θ_{ij} measures how far the relative angle between line-segments i and j is from a straight or right angle.

Then, line-segments are gradually extending in a kinetic framework which uses dynamic planar graph $G_t = (V_t, E_t)$ as underlying data-structure. Primitives, certificates and update operations are defined of kinetic formulation. Primitives correspond to half line-segments. For each primitive, certificate function $C_i(t)$ is defined as

$$C_i(t) = \prod_{\substack{j=1 \\ j\neq i}}^{N} \mathrm{Pr}_{i,j}(t) \tag{4}$$

where N is the number of primitives, and predicate function $Pr_{i,j}(t)$ returns 0 when primitive enters in collision with another primitive.

Update operations and more details about KIPPI are given in [10]. Before segmenting HSI $\mathcal{X} \in \mathbb{R}^{Q\times L\times B}$, where Q and L are the spatial dimensions, B is corresponding spectral band number, some preprocessing is required. In this work, the KIPPI is conducted on the first three components obtained by principal component analysis (PCA) to produce the partition results.

2.2. Training Sample Enlargement

To improve classification performance, the finest scale partition result obtained by KIPPI is utilized to search more reliable training samples. The finest scale partition result is defined as $\mathbf{P} = (\mathbf{p}_1, \mathbf{p}_2, \ldots, \mathbf{p}_n)$, n is the number of polygons. Furthermore, spectral angle mapper (SAM) is adopted to measure spectral similarity. Pixels with high spectral similarity are selected as the new samples.

The detailed procedures are described as follows:

1) Sample expansion in polygon: Finding the polygon $\mathbf{p}_t$ where single sample (also can be seen as target sample) is located in partition map. Then, spectral distance $\mathbf{D}_{ij}$ between different pixels $\mathbf{s}_i$ in $\mathbf{p}_t$ and target sample $\mathbf{s}_j$ is calculated as:

$$\mathbf{D}_{\mathrm{ij}} = \cos^{-1}\left(\frac{\sum_{i,j=1}^{B} s_i s_j}{\left[\sum_{i=1}^{B} s_i^2\right]^{\frac{1}{2}}\left[\sum_{j=1}^{B} s_j^2\right]^{\frac{1}{2}}}\right) \tag{5}$$

where B denotes the number of spectral bands. Sorting $\mathbf{D}_{ij}$ from smallest to largest, top 10% pixels are labeled as the same class with target sample.

2) Sample expansion between polygons: Objects belonging to the same class may distribute in different polygons. To search more samples which are not adjacent, the average spectral similarities of different polygons are calculated. Next, SAM is used to search the polygons which have high similarity with the target sample. Finally we calculate pixel-wise spectral distance between target sample and all pixels in these polygons. When distance is smaller than 0.01, the pixel is added to the training sample set.

After above procedures, the extended samples are sent to SVM for training. Then using SVM to classify the dimension reduced image $\mathcal{S}$ and obtain the initial classification result. It should be noted that $\mathcal{S} \in \mathbb{R}^{Q\times L\times \hat{B}}$ is acquired by PCA to the original HSI $\mathcal{X} \in \mathbb{R}^{Q\times L\times B}$. Moreover, $\hat{B}$ is fixed to 20 in this method.

2.3. Probability Optimization

In this step, the maximum probability rule is utilized to optimize the initial classification result obtained by SVM, which can model the spatial correlation between adjacent objects. Actually, the probability maps estimated by the SVM always

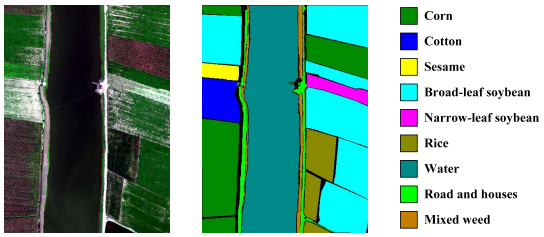

(a) (b) (c)

Fig. 2. WHU-Hi-LongKou data set. (a) Color composite. (b) Ground-truth. (c) Labels.

exist noise-like mislabeled pixels and are not consistent with the boundaries of objects in HSI because of lacking the spatial correlation. To alleviate this problem, multiscale partition results which contain various crops with different size, are used to remove the inhomogeneity within a regular cropland. Taking one partition result for example, the probability of different classes is counted in each polygon, when the maximum probability value is greater than 0.8, all pixels in the polygon are remarked as the corresponding class. Doing the same operation on all scales, multiscale classification results $\mathbf{R} = (\mathbf{R}_1, \mathbf{R}_2, \ldots, \mathbf{R}_M)$ are obtained, M is the number of different scale. Based on the maximum probability as follow, label of each pixel is determined.

$$\hat{R}_i = \arg\max_{\alpha} \left(\frac{1}{\mathbf{M}} \sum_{j=1}^{\mathbf{M}} f(\mathbf{R} \mid \alpha) \right) \tag{6}$$

$$f(\mathbf{R} \mid \alpha) = \begin{cases} 1, & \text{if } \mathbf{R}_{ij} \in \alpha \\ 0, & \text{otherwise} \end{cases} \tag{7}$$

where $\alpha = (1, 2, \ldots, c)$, c is the number of objects category.

3. EXPERIMENTAL SETTINGS AND RESULTS

3.1. Data Sets

In order to evaluate the classification performance of the proposed method, a new public HSI data sets, i.e., WHU-Hi-LongKou (crop scene) published in [11], is used here. This image contains 270 bands of size 550×400. Its false color image and ground truth are presented in Fig. 2.

3.2. Comparison Methods and Evaluation Metric

In this paper, we compare the proposed method with six state-of-the-art classification methods, including superpixel-based multiple kernels method [12] (SCMK), probabilistic-kernel collaborative representation with adaptive weighted graph based method [2] (PKAWG), PCA based edge-preserving features method [1] (PCA-EPF), multi-scale total variation based method [4] (MSTV), generalized tensor regression based method [3] (GTR) and random patches network based method [13] (RPNET). Furthermore, three commonly used measures, OA, AA, and Kappa coefficient, are adopted.

3.3. Experimental Results

The first experiment is performed on WHU-Hi-LongKou data set with single labeled sample per class. The samples are chosen randomly from the ground truth. Table 1 presents the accuracies of classification results obtained by different methods. These objective indexes are calculated by averaging the objective accuracies of 10 repeated experiments. It can be seen that the proposed method performs better than other methods in terms of objective indexes, with OA=82.65%, AA=77.68%, and Kappa=78.27%. Fig. 3 displays classification maps of all compared methods. Whether from visual effects or objective indicators to evaluate performance, the effectiveness of our method is conformed.

The second experiment analyses the classification accuracy of all methods with different initial training samples. Overall accuracy of corresponding experimental results are given in Fig. 4. As shown in Fig. 4, there is a positive correlation between the number of initial samples and accuracy. These compared methods could not obtain satisfactory results because of training sample set is very limited. However, our method is serviceable in this situation.

4. CONCLUSIONS

This paper proposed a novel hyperspectral image classification method for crop mapping with single training sample. The main advantage of our method is that the boundaries between different objects in the classification map are well aligned with the original image. Furthermore, the proposed method obtains satisfactory classification performance even when the training sample per class is one. It is also suitable for solving small labeled sample size problem. Besides, this method can be further improved by extracting more representative features.

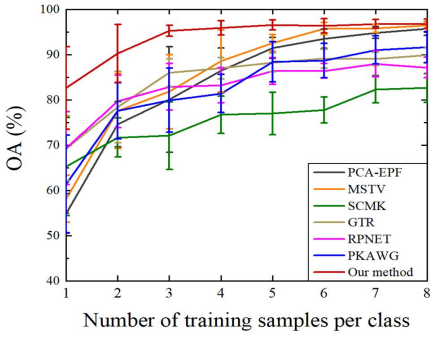

Fig. 4. OA as a function of the number of training samples for different methods.

Table 1. Classification performance of all studied methods for WHU-Hi-LongKou data set. The standard deviation (in the parentheses) of the accuracies obtained in repeated experiments is also reported.

Metrics	PCA-EPF [1]	MSTV [4]	SCMK [12]	GTR [3]	RPNet [13]	PKAWG[2]	Our method
OA(%)	54.92(4.32)	58.16(5.18)	55.46(8.66)	69.27(7.19)	69.33(8.03)	61.41(10.80)	**82.65**(9.12)
AA(%)	68.58(5.36)	69.19(4.37)	47.43(6.57)	57.85(8.45)	62.49(6.08)	53.71(7.10)	**77.68**(8.78)
Kappa(%)	39.56(5.86)	45.18(6.99)	46.53(9.36)	61.78(8.11)	62.80(9.02)	53.53(11.69)	**78.27**(10.76)

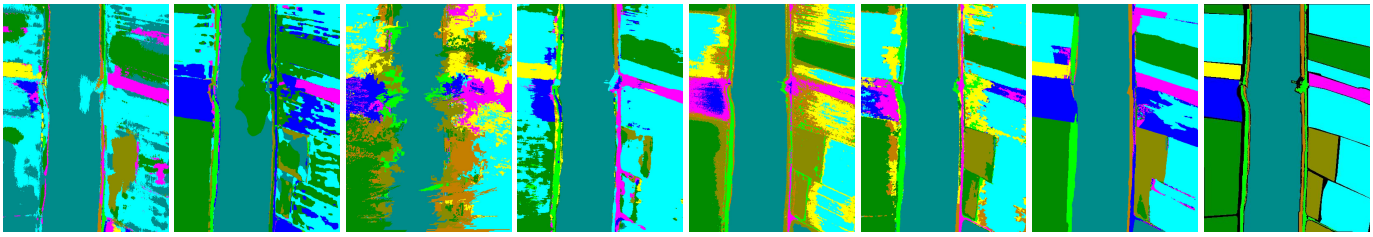

(a) PCA-EPF [1] (b) MSTV [4] (c) SCMK [12] (d) GTR [3] (e) RPNet [13] (f) PKAWG [2] (g) Our method (h) Ground-truth

Fig. 3. Classification results of different methods with single sample.

References

[1] X. Kang, X. Xiang, S. Li, and J. A. Benediktsson, "PCA-based edge-preserving features for hyperspectral image classification," *IEEE Trans. Geosci. Remote Sens.*, vol. 55, no. 12, pp. 7140–7151, 2017.

[2] J. Liu, Z. Wu, J. Li, A. Plaza, and Y. Yuan, "Probabilistic-kernel collaborative representation for spatial–spectral hyperspectral image classification," *IEEE Trans. Geosci. Remote Sens.*, vol. 54, no. 4, pp. 2371–2384, 2015.

[3] J. Liu, Z. Wu, L. Xiao, J. Sun, and H. Yan, "Generalized tensor regression for hyperspectral image classification," *IEEE Trans. Geosci. Remote Sens.*, vol. 58, no. 2, pp. 1244–1258, 2019.

[4] P. Duan, X. Kang, S. Li, and P. Ghamisi, "Noise-robust hyperspectral image classification via multi-scale total variation," *IEEE J. Sel. Top. Appl. Earth Observ. Remote Sens.*, vol. 12, no. 6, pp. 1948–1962, 2019.

[5] M. Zhang, M. Gong, Y. Mao, J. Li, and Y. Wu, "Unsupervised feature extraction in hyperspectral images based on wasserstein generative adversarial network," *IEEE Trans. Geosci. Remote Sens.*, vol. 57, no. 5, pp. 2669–2688, 2018.

[6] L. Wang, S. Hao, Q. Wang, and Y. Wang, "Semi-supervised classification for hyperspectral imagery based on spatial-spectral label propagation," *ISPRS J. Photogramm. Remote Sens.*, vol. 97, pp. 123–137, 2014.

[7] K. Tan, J. Hu, J. Li, and P. Du, "A novel semi-supervised hyperspectral image classification approach based on spatial neighborhood information and classifier combination," *ISPRS J. Photogramm. Remote Sens.*, vol. 105, pp. 19–29, 2015.

[8] J. Li, J. M. Bioucas-Dias, and A. Plaza, "Spectral–spatial classification of hyperspectral data using loopy belief propagation and active learning," *IEEE Trans. Geosci. Remote Sens.*, vol. 51, no. 2, pp. 844–856, 2012.

[9] Z. Wang, B. Du, L. Zhang, and L. Zhang, "A batch-mode active learning framework by querying discriminative and representative samples for hyperspectral image classification," *Neurocomputing*, vol. 179, pp. 88–100, 2016.

[10] B. Jean-Philippe and L. Florent, "KIPPI: Kinetic polygonal partitioning of images," in *2018 IEEE Conference on Computer Vision and Pattern Recognition (CVPR)*, 2018, pp. 3146–3154.

[11] Y. Zhong, X. Hu, C. Luo, X. Wang, J. Zhao, and L. Zhang, "Whu-Hi: UAV-borne hyperspdectral with high spatial resolution (H2) benchmark datasets and classifier for precise crop identification based on deep convolutional neural network with CRF," *Remote Sens. Environ.*, vol. 250, pp. 112012, 2020.

[12] L. Fang, S. Li, W. Duan, J. Ren, and J. A. Benediktsson, "Classification of hyperspectral images by exploiting spectral-spatial information of superpixel via multiple kernels," *IEEE Trans. Geosci. Remote Sens.*, vol. 53, no. 12, pp. 6663–6674, Dec. 2015.

[13] Y. Xu, B. Du, F. Zhang, and L. Zhang, "Hyperspectral image classification via a random patches network," *ISPRS J. Photogramm. Remote Sens.*, vol. 142, pp. 344–357, 2018.